Astragalus Polysaccharide Regulates EGFR and ANXA1 Expression to Inhibit Tumor Growth

Wenfang Li
School of Life Science and Technology
Xueyan Hu
State Key Laboratory of Fine Chemicals
Yanjie Li
School of Pharmacy
kedong song (kedongsong@dlut.edu.cn)
Dalian University of Technology https://orcid.org/0000-0003-2185-1050

Research

Keywords: Astragalus polysaccharide, Cell cycle, Cell apoptosis, EGFR, ANXA1

Posted Date: February 23rd, 2021

DOI: https://doi.org/10.21203/rs.3.rs-221757/v1

Abstract

Background: Astragalus polysaccharide (APS) has been frequently used as an adjuvant agent responsible for its immunoregulatory activity to enhance efficacy and reduce toxicity of chemotherapy used in the management of breast cancer. However, the other synergism mechanism of APS remains unclear.

Methods: The expression profiles of breast cancer biological data (E-GEOD-10780), (E-GEOD-65194), (E-GEOD-10810), (E-GEOD-42568), (E-GEOD-61304), (E-GEOD-7904) and (E-GEOD-15852) were retrieved from European bioinformatics institute (EBI) database to identify differentially expressed genes (DEGs). Gene Ontology and pathway enrichment analyses were carried out. The protein–protein interaction (PPI) networks of the DEGs were constructed by STRING online database. Finally, STRING was applied to construct the PPI networks of the DEGs associated with cell proliferation, cell cycle and cell apoptosis from GO enrichment analysis. Subsequently, hub and common genes that might be the potential targets and possible mechanism behind APS *in vivo* direct anti-tumor activity on breast cancer were identified. Meanwhile, we evaluated the mRNA and protein expression levels of these key targets using multiple biological analyses.

Results: In total, 116 down-regulated and 73 up-regulated differential expressed genes (DEGs) were examined from seven gene expression datasets. Top ten hub genes were obtained in four typical protein-protein interaction (PPI) network of DEGs involved in each specific biological process (BP, cell cycle, cell proliferation, cell apoptosis and death) that was related to inhibitory activity of APS *in vitro* against breast cancer cell lines. Four common DEGs (EGFR, ANXA1, KIF14 and IGF1) were further identified in the above four BP-PPI networks, among which EGFR and ANXA1 were the hub genes that were potentially linked to the progression of breast cancer. The results of biological detections indicated that APS could down-regulated EGFR and up-regulated ANXA1 expression.

Conclusion: In conclusion, the present study may provide potential molecular therapeutic targets and a new insight into the mechanism of APS against breast cancer.

Introduction

Breast cancer is one of most commonly diagnosed cancers in women all around the world. Despite the remarkable advancements in the detection and treatment of breast cancer, it remains the most life-threatening disease accounted for 25% of all cancers in women [1]. The exploration of novel therapeutic agents with preferable efficacy and low toxicity is urgently needed for breast cancer treatment. Currently, several polysaccharides have been developed and attracted growing interests in the adjuvant therapy of various carcinomas since they are effective or sensitize chemotherapy contributing to improve quality of life and patient survival [2].

Astragalus polysaccharide, the main active ingredient extracted from the natural product astragalus membranaceus, has been considered as a good candidate for adjuvant treatment of cancer owing to its

low toxic, immunomodulatory and anti-tumor properties [3]. APS mainly exert anti-tumor effects via the following ways: immune system enhancement, direct cytotoxicity, and synergistic effects in combination with chemotherapy. Extensive studies have been investigated the tumor-killing capability of APS in multiple tumor types [4, 5]. Ye et al indicated that APS could inhibit the proliferation of breast tumor cell line by up-regulating the expressions of p53 and PTEN [6]. APS combined with vinorelbine and cisplatin was reported to increase tumor response, significantly improve performance status of patients in advanced non-small-cell lung cancer [7]. It has been evident from various animal studies and clinical trials that APS produces indirect cytotoxicity or promotes host immune response in combination with other chemotherapeutic drugs [8, 9]. Beside this, the other underlying molecular anti-cancer mechanism of APS remains unclear.

It is inevitable to assess the *in vivo* anti-tumor potential of APS by enhancing immune functions of host organism with suitable animal models. However, the immune system is relatively complex and the efficacy of tests *in vivo* displayed through immune system will emerge slowly after at least 3 weeks [10]. Consequently, it is time- and cost-consuming and difficult to explore the specific immune-regulation mechanism of APS against breast carcinogenesis. The introduction of bioinformatics analysis to evaluate the essential genes involved in the development of breast cancer provides a value prediction that is efficient and less loss in clinical expense prior to the following experimental verification [11].

Previous studies performed in our lab investigated the anti-cancer potentials of APS towards 4T1-solid tumor and breast cancer cell lines both *in vivo* and *in vitro*, mainly by enhancing immune response, coordinating chemotherapy drugs, inducing apoptosis, arresting cell cycle and inhibiting cell proliferation [8, 12]. To discover the underlying anti-cancer molecular mechanism of APS, we employed bioinformatics approaches to find out differentially expressed genes (DEGs) of normal and breast tumor tissues. Additionally, these DEGs underwent Gene ontology (GO)/Kyoto Encyclopedia of Genes and Genomes (KEGG) pathway enrichment and protein-protein interaction (PPI) network construction. In especial, representative DEGs were screened out involved in biological processes (BPs, cell cycle, cell proliferation and cell apoptosis) to further construct BPs-PPI networks. The common hub genes were picked out followed by multiple experimental validations to reveal the potential targets and mechanism of APS against breast cancer. We found that the inhibitory activity of APS towards 4T1-solid tumor may be associated with the regulation of EGFR and ANXA1 (Figure.1).

Materials And Methods

Materials and regents

The green fluorescent protein (GFP)-labeled and luciferase-labeled 4T1 cells used in the study were purchased from Mingjin Energy Technology Co., Ltd. (Shanghai, China). The required medium was renewed at regular basis after 2 days. When the cells confluence was 80–90% then a passage was required. Astragalus polysaccharide was obtained from Pharmagenesis Inc. (Beijing, China). 5-fluorouracil (5-FU) was acquired from Sigma Aldrich Co. (St Louis, MO, USA). Fatal bovine serum (FBS),

trypsin-EDTA, RPMI-1640 medium and penicillin–streptomycin were obtained from Gibco (Grand Island, NY, USA). The anti- ANXAI and Anti-EGFR antibody was obtained from Abcam Inc. (Cambridge, MA, USA). All the necessary chemicals utilized in the study, were of analytical grade.

Identification of DEGs

Microarray expression profile breast cancer biological data (E-GEOD-10780), (E-GEOD-65194), (E-GEOD-10810), (E-GEOD-42568), (E-GEOD-61304), (E-GEOD-7904) and (E-GEOD-15852) were retrieved from European bioinformatics institute (EBI) database, which was comprised of 251 normal samples and 483 breast cancer samples. RMA algorithm in Affy package was performed to preprocess the raw expression data in the R statistical software consist of background correction, medianpolish summarization and quantile normalization methods. Furthermore, SAM method (significance analysis of the microarrays) was used for the assessment of differentially expressed genes between normal and BC samples.

Functional and pathway enrichment analysis

To describe the biological characteristics and functional annotation of DEGs, Go and KEGG pathway enrichment analysis were performed using Database for Annotation, Visualization and Integrated Discovery (DAVID, https://david.ncifcrf.gov/)[13] online tool. $P < 0.05$ was set as the cut-off criterion.

Construction of PPI network and hub gene selection

The online database Search Tool for the Retrieval of Interacting Genes (STRING, http://string.embl.de/) was employed to build up PPI network of DEGs, for the assessment of considerably important linkage between DEGs. Besides, another PPI network of the DEGs was also constructed in the first six KEGG pathways with the most significant difference. The confidence score ≥ 0.2 was set as the cutoff criterion. For the visualization of PPI network Cytoscape 3.5.1 software was used.

The previous findings in our lab indicated that the activated macrophages by APS *in vitro* could inhibit the progress of breast cancer cells via cell cycle arrest, inhibiting cell proliferation and promoting cell apoptosis [8, 12]. Specially, STRING was applied to construct the PPI networks of the DEGs associated with cell proliferation, cell cycle and cell apoptosis from GO enrichment analysis. Subsequently, hub genes were determined on the basis of degree > 10 by cytoHubba plugin, the common genes were identified from the PPI network constructed by the DEGs involved in the above biological processes.

Transplanted tumor and treatment protocol

A sum of 60 female BALB/c mice (18-22g, 6 ~ 8 weeks old) were obtained from Dalian Medical University (Dalian, China) and were housed at 25 ± 1°C in 50–60% humidity under a 12 h dark/light cycle. Tumor was transferred to the healthy mice by injecting 1.5×10^6 of the GFP-4T1 cells, targeting the female BALB/c mice right flunk area. Besides, the equal numbers of 4T1-luc cells were injected to evaluate tumor progress and drug efficiency using live animal imaging. When the tumor was extended to a size of $100mm^3$, all animals were randomly allocated to five groups (n = 10/group) as follows: (I) Negative control group: intraperitoneal injection with 0.1 ml normal saline; (II) a low dose APS group:

intraperitoneal injection with 100 mg/kg/d APS; (III) a high dose APS group: intraperitoneal injection with 200 mg/kg/d APS; (IV) 5-FU group: intraperitoneal injection with 20 mg/kg/d 5-FU as a positive control; (V) combined group: the mice were administered APS at 200 mg/kg/d and 5-FU at 20 mg/kg/d, once daily. Using Vernier caliper scales the volume of existing tumor was measured regularly every next day, and was calculated with the following equation: length × width^2 × 0.5. After fourteen days, live animal imaging was conducted to observe the effects of APS on the development of subcutaneous tumors *in vivo* using IVIS Spectrum imaging system (PerkinElmer, MA, USA). Mice were anesthetized with 3.5% chloral hydrate and real-time images were taken and further analyzed using the Living Image 3.1 software. Afterwards, the mice were killed all together, and the tumors were excised, fixed in formalin (10%), and were embedded in paraffin for subsequent studies.

Cell viability evaluation

Live/dead staining and CCK-8 analysis were performed to assess the viability of GFP-4T1 cells sorted from *in vivo* tumors after 14 days of drug treatment. In brief, GFP-4T1 cells were harvested after the excisional tumor tissues were underwent cutting, digestion with collagenase, filtration with 200 mesh filter, erythrocytes removal with lysate. GFP-4T1 cells were sorted using FACS Aria III cell sorter (BD Biosciences, USA). Upon overnight adherent culture, 4T1 cells in each group were incubated with calcein-AM(2 μmol/L), propidium iodide (PI, 4 μmol/L), and Hoechst 33342 staining (5μg/L) in PBS at 37°C for 15 min. Afterwards, cells were imaged with an inverted fluorescence microscope. Besides, CCK-8 analysis was conducted to evaluate cell viability as previously described [14]. The optical density value of each group was measured at a wavelength of 450 nm using an iMark microplate reader (Bio-Rad, CA, USA).

Quantitative real-time PCR analysis

To evaluate the mRNA expression of EGFR and ANXAI, quantitative real-time RT-PCR was conducted. Using RNAiso Plus kit (Takara Biotechnology Co. Ltd, Dalian, China), the total RNA was extracted in accordance to the manufacturer's instructions. With the help of a PrimeScript™ RT reagent Kit (Takara Biotechnology Co. Ltd, Dalian, China) cDNA was synthesized from RNA by considering the following temperature protocol: 25°C for 10 min, 42°C for 50 min and 80°C for 10 min. PCR analysis was conducted in an ExicyclerTM 96 real-time PCR instrument (Bioneer, Daejeon, Korea) for 40 cycles (94°C for 10 s, 60°C for 20 s, 72°C for 30 s) after initial denaturation at 94°C for 5 minutes, utilizing the TransScript™ SYBR® Green Master Mix kit (Takara Biotechnology Co. Ltd, Dalian, China). The expression level was determined as a ratio between the internal control β-actin and hub genes occurring in the same sample of mRNA, and was calculated by the comparative CT method. The 2-ΔΔCt method was used for the calculation of relative mRNA fold changes. The primers of hub genes were synthesized by GenScript Biotech Corp. (Nanjing, China), and their sequences were given in Table 1.

Table 1
Primer information for the RT-PCR

Gene	Forward primer	Reverse primer
EGFR	5'-CCAAGGCACGAGTAACAAGC-3'	5'-AGGGCAATGAGGACATAACCAG-3'
ANXA1	5'-GGGTGACCGATCTGAGGAC-3'	5'-CTGGTGGTAAGGATGGTATTG-3'
β-actin	5'-CTTAGTTGCGTTACACCCTTTCTTG-3'	5'-CTGTCACCTTCACCGTTCCAGTTT-3'

Immunohistochemical analysis

Immunohistochemical (IHC) analysis was conducted to assess the APS effects on the expression of key proteins in 4T1 cells and analyze anti-cancer mechanism of APS based on bioinformatic approach. Briefly, paraffin-embedded tumor sections (5 μm) were deparaffinized, rehydrated and boiled in a citrate buffer solution for antigen retrieval. Tumor sections were incubated in 3% H_2O_2 and blocked with goat serum. Subsequently, the samples were incubated with antibodies for EGFR and ANXA1 at 4°C overnight, followed by being incubated with goat anti-rabbit (HRP), stained with DAB chromogen and counterstained with hematoxylin. All sections were observed, using light microscope (Olympus, Tokyo, Japan). A semi-quantitative analysis of the IHC images was performed by utilizing the Image-Pro Plus 6.0 (IPP, Media Cybernetics, USA) software.

Immunofluorescence and flow cytometry assay

Immunofluorescence (IF) and flow cytometry assays were conducted to evaluate the expression of EGFR and ANXA1 proteins in GFP-4T1 cells sorted from subcutaneous tumors after treatment with APS for 14 days. GFP-4T1 cells were harvested and cultured for adhesion. Cells were fixed with 4% paraformaldehyde for 20 min, permeabilized at 0.1% Triton X-100 for 30 min and blocked with 10% goat serum in PBS for 60 min. Subsequently, cells were incubated with primary antibody (EGFR, ANXA1, 1:100) overnight at 4°C prior to incubation with second antibody (Cy3, 1:100) at room temperature for 1h and counterstaining with DAPI at 37°C for 15 min. Images were taken using a laser confocal microscope (FV1000, Olympus, Japan). Besides, the expressions of EGFR and ANXA1 were analyzed using flow cytometry as described above except for adding centrifugation before each procedure. All flow cytometry data were analyzed with **FlowJo7.6.2** (Tree Star, San Carlos, CA, USA).

Statistical analysis

All the results of this study were presented as mean ± SD. A one-way analysis of variance (ANOVA) was used for the comparison of the means among the different groups. Moreover, a significant difference of $P < 0.05$ was also noted. With the help of Origin 8.0 software (Origin Lab, MA, USA) and GraphPad Prism Version 5.0 software (GraphPad Software Inc., San Diego, CA, USA), all of the statistical analysis were carried out.

Results

The identification of DEGs

We downloaded seven gene expression datasets from EBI database including 483 breast cancer samples and 251 normal samples. Sums of 201 genes were screened to be differentially expressed genes. Furthermore, 189 genes were identified as the uniformly regulated genes after selecting the intersections of differential gene sets, among which 73 genes were upregulated and 116 genes were downregulated (Table 2).

Table 2
Common up-regulated and down-regulated DEGs in the seven breast cancer data

Down-regulated Gene		Down-regulated Gene		Up-regulated Gene		Up-regulated Gene
ADAMTS5	PLSCR4	ECM2	S1PR1	NUSAP1	FEN1	PCNA
SPRY2	SOBP	RBP4	VWF	ECT2	STAT1	PARP1
DMD	CEP68	SVEP1	TACC1	RRM2	BUB1B	GARS
FOXO1	ACACB	ANK2	BNIP3L	RACGAP1	AURKA	STMN1
NDN	TNS1	MFAP4	LIPE	COL11A1	CDC20	ACOT7
ABCA8	MAFF	SIK2	SLIT3	COL10A1	TYMS	ORC6
LMOD1	PDZRN3	ANXA1	FMOD	DTL	CXCL9	DDX39A
FAM13A	PLIN1	IGF1	CD248	TOP2A	NCAPG	DYRK2
EDNRB	IL11RA	CFH	TIMP4	UBE2C	ISG15	ACTL6A
CAV2	GPC3	ADIPOQ	FHL1	KIAA0101	PBK	TRIM14
SORBS1	CLDN5	LEP	PCSK5	CENPU	GINS2	TRIM14
ADH1B	AOC3	FABP4	CD36	CKS2	EZH2	CKAP4
HLF	SASH1	ITGA7	APOLD1	NEK2	DLGAP5	E2F3
TGFBR3	ADAMTS1	PALMD	ATP1A2	CCNB1	SMC4	
DLC1	DCN	MEOX1	ABLIM3	PTTG1	SLC7A5	
SRPX	ENPP2	AKAP12	TNMD	ZWINT	RFX5	
IGFBP6	CDKN1C	MEOX2	BHMT2	HMGB3	CTPS1	
IRS2	COX7A1	GPD1	ITSN1	RABIF	TBCE	
CFD	AMOTL2	CES1	CA4	INHBA	CENPN	
GNG11	MT1X	LAMA4	F10	PRC1	KIF14	
CAV1	PDE2A	EGFR	TEK	CXCL10	CCNA2	
LHFP	FOSB	GYG2	SERPING1	MELK	MFAP2	
CDO1	NRN1	HSPB2	CDH5	S100P	UBQLN4	
RGL1	ZBTB16	EHD2	ACSM5	MAD2L1	RSAD2	
FMO2	TGFBR2	FGF2	PARVA	GINS1	WDYHV1	
SEMA3G	ARHGEF6	ASPA	SLC19A3	CENPF	SNRPG	
PTRF	PPP1R1A	MXRA7		ASPM	MCM2	

Down-regulated Gene		Down-regulated Gene	Up-regulated Gene		Up-regulated Gene
EZH1	DPT	NR3C1	CEP55	CDC7	
CXCL12	G0S2	ARHGEF40	HMMR	INTS8	
MAOA	CIDEC	ERG	SULF1	MTHFD2	

GO functional annotation and KEGG pathway enrichment analysis of DEGs

To explore in detail the function of these DEGs in BC, GO terms including biological process (BP), molecular function (MF), and cell component (CC) were evaluated by utilizing DAVID. It has been revealed from the results that DEGs were specifically enriched in certain biological processes, including cell division, cell cycle, chromosome segregation and cell proliferation (Fig. 2). As to CC, DEGs were primarily enriched in cytoplasm, membrane, cytoskeleton and proteinaceous extracellular matrix. For MF, DEGs were profoundly enriched in protein binding, glycosaminoglycan binding, receptor binding and heparin binding. All changes of these functional enrichments are closely associated with the adhesion, growth, metastasis, invasion and proliferation of tumor cells. On this basis, the occurrence and development of tumors result from the comprehensive regulation of multiple pathways with network structure rather than the action of single or several pathways.

In order to evaluate the 201 DEGs for the enrichment of KEGG pathway, DAVID was used, and the results were shown in Fig. 3a and Table 3. KEGG pathways results indicated that the DEGs were predominantly enriched in cell cycle (12 genes), AMPK signaling pathway (9 genes) and pathways in cancer (14 genes). In addition, the subnetworks of the top six pathways including cell cycle, AMPK signaling pathway, pathways in cancer, ECM-receptor interaction, proteoglycans in cancer and focal adhesion were constructed by STRING software (Fig. 3b), which intuitively presented the direct connection between the different genes enriched in each pathway.

Table 3
Twelve significant (P < 0.05) KEGG pathways

Path ID	Path term	P value
hsa04110	Cell cycle	3.60×10^{-6}
hsa04152	AMPK signaling pathway	6.99×10^{-4}
hsa05200	Pathways in cancer	0.0089
hsa04512	ECM-receptor interaction	0.0120
hsa05205	Proteoglycans in cancer	0.0137
hsa04510n	Focal adhesion	0.0162
hsa05212	Pancreatic cancer	0.0193
hsa04068	FoxO signaling pathway	0.0193
hsa03320	PPAR signaling pathway	0.0213
hsa04610	Complement and coagulation cascades	0.0235
hsa04920	Adipocytokine signaling pathway	0.0245
hsa04114	Oocyte meiosis	0.0310

PPI network construction and hub gene selection of DEGs involved in specific biological process

Here, the PPI network of 189 DEGs (simultaneous up-regulation or down-regulation) was constructed with 146 nodes and 733 edges by STRING database (Fig. 4a). A total of 56 genes in the BPs associated with cell cycle, cell proliferation, cell apoptosis and death were constructed to the BP-PPI network that containing 56 nodes and 267 edges (Fig. 4b). In addition, four PPI networks of the involved DEGs in each representative BP were built as shown in Fig. 4c I - IV. The top ten genes with high degree score were presented in these 4 BPs, among which 7 genes were remarkably identified (degree > 45) such as CCNB1, DLGAP5, CDC7, CSE1L, GINS1, AURKA and ECT2, suggesting their dominant roles in the regulation of the proliferation or apoptosis of breast cancer cells.

Common gene selection of DEGs in specific BP-PPI network

The PPI network of the DEGs strongly connected with the 4 representative biological processes was further constructed and 4 common genes were identified including EGFR, ANXA1, KIF14 and IGF1 after the division of DEGs in each BP as shown in Fig. 5 (blue square). Of particular note, EGFR (degree = 16) and ANXA1 (degree = 15) were also the hub genes in the 4 BP-PPI networks as presented in Table 4, indicating their particular importance in the enhancement of breast cancer cell apoptosis and

progression. Thus, key targets EGFR and ANXA1 were identified for experimental verification to study the possible mechanism of anti-breast cancer of APS.

Table 4
Top 10 DEGs with high degree in four typical BP-PPI networks

Cell cycle		**Cell proliferation**		**Apoptotic process**		**Cell death**	
Gene	Degree	Gene	Degree	Gene	Degree	Gene	Degree
CCNB1	60	CCNB1	68	AURKA	53	AURKA	53
CDC7	47	DLGAP5	48	ECT2	48	ECT2	48
E2F3	19	CDC7	47	CSE1L	46	CSE1L	46
EGFR	16	CSE1L	46	NR3C1	23	NR3C1	23
ANXA1	15	GINS1	45	**EGFR**	16	**EGFR**	16
EZH2	15	PCNA	19	**ANXA1**	15	**ANXA1**	15
PRC1	14	E2F3	19	MCM2	14	MCM2	14
CCNA2	14	**EGFR**	16	TOP2A	14	TOP2A	14
ASPM	14	TYMS	15	BUB1B	13	BUB1B	13
CDC20	13	**ANXA1**	15	MAD2L1	13	MAD2L1	13

Effect of APS on the expression of EGFR and ANXA1

The results of live animal imaging demonstrated that tumor volumes markedly decreased with the intervention of APS for 14 days as compared to that in negative control group (Fig. 6a). Besides, APS inhibited tumor growth evidenced by the tumor appearance and significantly depressed tumor weight (Fig. 6b-c). In addition, GFP-4T1 cells were sorted from subcutaneous tumors in BALB/c mice after treatment with APS for 14 days. Upon incubation overnight, live/dead staining indicated that the number of living GFP-4T1 cells reduced, while the number of dead cells increased in APS groups (Fig. 6d). CCK-8 analysis showed APS (200mg/kg) significantly decreased cell viability as compared to that in untreated group ($P < 0.001$). Further, it's more cytotoxic of APS towards 4T1 cells when combined with 5-FU ($P < 0.001$, Fig. 6e). All these results demonstrated the growth-inhibiting effect of APS on 4T1-solid tumor.

In this study, we further examined whether the inhibition of tumor growth *in vivo* by APS was associated with the regulation towards EGFR and ANXA1. The mRNA and protein expression of the ANXA1 and EGFR were measured by RT-PCR and IHC. Upon treatment with APS, the positive expression of ANXA1 protein increased, while the level of EGFR protein decreased in 4T1 solid tumors, especially in the high dose APS group. The trends of increased and decreased expression of two proteins in breast cancer tissues were more remarkable in the combined group (Fig. 7a). The results of RT-PCR and semi-quantitative evaluation of IHC revealed that APS treatment profoundly up-regulated the expressions of ANXA1 mRNA and protein

comparatively to that in negative control group ($P < 0.05$, Fig. 7b-c). On the contrary, APS administration markedly down-regulated the expression of EGFR mRNA and protein compared with that in negative control group ($P < 0.05$, Fig. 7b-c).

Post analysis for the sorted GFP-4T1 cells from subcutaneous tumors in BALB/c mice, the results of flow cytometry analysis revealed that decreased percentage of GFP-4T1 cells from solid tumors was identified in APS groups compared with that in untreated group (Fig. 8a), which also suggested the anti-tumor activity of APS. Post overnight culture, IF and flow cytometry assays were further performed to study the expression of EGFR and ANXA1 proteins from the sorted GFP-4T1 cells. Note that morphologic changes between non-labeled and GFP-labeled 4T1 cells. GFP-4T1 cells showed a contracted morphology and were prone to aggregate growth, while non-labeled 4T1 cells were flatter (Fig. 8b). Decreased expression of EGFR in 4T1 cells was observed after exposure to APS, particularly in combination with 5-FU (Fig. 8c, e), while the expression of ANXA1 was increased after undergoing APS and combined treatment (Fig. 8d, e). Meanwhile, DAPI staining showed APS induced cell apoptosis with nuclear chromatin condensation and nuclear fragmentation (white arrow, Fig. 8d). APS (200mg/kg) significantly down-regulated EGFR expression and up-regulated ANXA1 expression compared with that in negative control group ($P < 0.01$, Fig. 8f). All these findings indicated that the regulation of EGFR and ANXA1 in 4T1 solid tumor may be the underlying anti-cancer molecular mechanism of APS in addition to or following the improvement of the immune function.

Discussion

Recently, APS has attracted growing interests in biological fields especially in terms of cancer therapy. Most of studies have clarified that APS inhibit tumor growth through immunopotentiation activity and generally be considered as a powerful adjunctive strategy in combination with chemotherapy for various tumors [15, 16]. There are also parts of studies suggest the direct anti-tumor activity of APS, such as the inhibition of cell proliferation, the induction of cell apoptosis and cell cycle arrest [17, 18]. In the present study, for the first time, we employed bioinformatics approach to specifically target the common hub genes involved in the *in vitro* anti-tumor biological processes, and further underwent experimental verification. The aim of this study was to explore other possible anti-tumor mechanisms of APS and to find the potential therapeutic targets for breast cancer.

KEGG pathways analysis demonstrated that the DEGs were mainly enriched in cell cycle, AMPK signaling pathway and pathways in cancer, which are potentially associated in the progression of breast tumor and used as the regulating target for cancer treatment [19, 20]. For instance, downregulation of AMPK activity or decreased expression appear to promote breast tumorigenesis, while AMPK activation was found to impede tumor growth. Pan et al showed that cetyl trimethyl ammonium bromide could enhance DOX chemosensitivity mainly through activation of AMPK signaling cascades in breast cancer [21]. Another report found that targeting AMPK alpha signaling was capable of improving radiosensitivity of triple negative breast cancer [22]. All these potentially enriched pathways will contribute to identify important molecules involved in the growth of breast cancer.

It is more meaningful to study the mechanism of tumor progression by classifying the genes involved in the same function or pathway using GO functional annotation. In this study, PPI networks of all DEGs and corresponding DEGs in four BPs including cell cycle, cell proliferation and cell apoptosis were specially constructed and the hub nodes were selected in all PPI networks. Such treatment focused on the biological process network pathway of differential genes associated with breast cancer rather than being confined to individual genes to study the expression changes of key genes or proteins throughout the entire pathway. Here, the hub nodes were purposefully analyzed in PPI networks constructed by DEGs in 4 typical BPs (cell cycle, cell proliferation, cell apoptosis and death) because they were involved in the anti-cancer mechanism of APS mediated macrophages in our previous study [12, 23]. Moreover, the regulatory genes of cell cycle are frequently linked to the incidence and growth of tumor, which are mutated under the action of carcinogenic factors, causing the disorder of cell cycle followed by the malignant proliferation of cells and tumor formation [24, 25]. It has been extensively acknowledged that cell apoptosis plays a potential role in the inhibition of tumor growth, or it may develop resistance to tumor progression [26, 27]. Further, tumor cell death induced by most of anti-cancer strategies is directly related to the activation of apoptosis. On this basis, the main focus of this study was to investigate the hub genes in the four BP-PPI networks to explore other possible anti-breast cancer mechanisms using bioinformatics based on previous findings in our lab.

In this study, a sum of 56 genes in the four BP-PPI networks, among which 7 genes (CCNB1, DLGAP5, CDC7, CSE1L, GINS1, AURKA and ECT2) were particularly significant with the degree over 45. For these genes, CCNB1 is essential for controlling the cell cycle at the G2/M transition, which has been displayed in multiple cancer types playing important roles in the promotion and transformation of tumor [28]. DLGAP5 and CDC7 are potential cell cycle regulators that play roles in carcinogenesis of cancer cells. Elevated expressions of DLGAP5 were noticed in breast cancer specimens and were associated with poor prognosis [29]. Moreover, a cellular apoptosis susceptibility protein (CSE1L), is extensively expressed in certain types of cancers. Mounting evidences from several pathological reports have been indicated that highly expressed CSE1L are most frequently associated with the tumor proliferation [30]. Tai et al indicated that CSE1L was of paramount importance in facilitating tumor cells apoptosis imparted by chemotherapeutic agents and could also regulate the metastasis and invasion of breast cancer [31]. Accumulating evidence has indicated that the aberrant expression of GINS1 was involved in cancer pathogenesis [32]. Breast cancer patients with elevated expression of GINS1, have been predicted with significantly poor prognosis, however the knockdown of GINS1 could inhibit the malignant features of breast cancer cells [33]. AURKA is involved in regulating many early mitotic events that also plays an important role in tumorigenesis and tumor progression. Extensive studies have demonstrated that AURKA was overexpressed in certain types of malignancies, such as bladder cancer, esophageal squamous cell carcinoma and breast cancer [34, 35]. It is evident from previous studies that ECT2 can improve cell growth, invasion and tumorigenicity [36]. All these findings demonstrate the vital roles of these genes in the progression of breast cancer, and will be verified in our further study.

Previous study in our lab demonstrated that the *in vivo* the inhibitory activity of APS towards 4T1-solid tumor was partially associated with the enhancement of immune responses [8]. Here, the other *in vivo*

underlying molecular mechanism of APS against breast cancer was further studied using bioinformatics method targeting *in vitro* anti-tumor strategies. In the present study, common hub genes EGFR and ANXA1 were identified in biological processes involving in cell cycle, cell proliferation and cell apoptosis targeting to the inhibitory mechanism of APS mediated macrophages against breast cancer cells. Correspondingly, IHC and PCR were carried out to study the effect of APS on the proteins and genes expression of EGFR and ANXA1, respectively. Currently, accumulating evidences have demonstrated that EGFR and ANXA1 are aberrant expression in multiple tumors [37, 38]. EGFR, a transmembrane glycoprotein, belongs to the extracellular protein ligand of the epidermal growth factor family that is involved in a myriad of biological processes and carcinogenic events. It can be used as a tumor marker for serological detection. Significant difference of EGFR expression was identified in the serum of healthy people and gastric cancer patients [39]. EGFR can be detected in the serum of patients with early-stage gastric cancer, which thus can be used as one of the screening indicators for high-risk groups. Up-regulated EGFR protein and transcript levels were related to poor prognosis in various cancers, including colorectal cancer, endometrial cancer and non-small cell lung cancer [40]. Besides, EGFR is also a hot target and predictive indicator of early recurrence and death of breast cancer. The degree of EGFRs high expression determines the amount of the down regulation, which occurs in the natural functions of family members (ErbB4/Her4, ErbB3/Her3, ErbB1/EGFR1 and ErbB2/Her2) and their use as indicators for clinical outcome in breast cancer and other tumor types [41]. The study reported that the high levels of surface tyrosine kinase receptors of EGFR family were frequently found in breast cancers [42]. The overexpression of EGFR was identified in approximately 40% of triple-negative breast cancer (TNBC) patients that provide a potential strategy for targeting TNBC therapy [43]. The result of EGFR with high degree indicated its significant role in the progression of breast cancer and reflected the feasibility of PPI analysis.

ANXA1 refers to the first protein found in the Annexins family that plays an extremely vital role in tumor proliferation and differentiation, inflammatory response, cell signal transduction, calcium ion signaling channels, and interactions between cytoskeletal proteins [44]. Currently, numerous reports have demonstrated differential expression of ANXA1 depending on cancer type. Several studies have reported higher levels of ANXA1 in esophageal cancer, skin squamous cell carcinoma and colorectal cancer, while others have reported decreased expression of ANXA1 in head and neck cancer, prostate cancer, oral squamous cell carcinoma and cervical cancer [45]. Significant down-regulation of ANXA1 protein was identified in esophageal squamous cell carcinoma compared with that in paracancerous normal tissue [46]. Notably, there are contradictory reports about the role of ANXA1 plays in breast cancer. Mussunoor et al indicated that the over expression of ANXA1 was found in triple negative breast cancer and metastatic cancer, which plays a prominent role in tumor progression and development [47], while another report showed that ANXA1 was downregulated during late stage of progression and metastasis in breast cancer [48]. Using high-throughput analysis and also evidenced by IHC and RT-PCR that the event of decreased expression of ANXA1 occurs in the human breast cancer [49]. Besides, previous report showed that the expression of ANXA1 remarkably decreased in breast tumor including ductal carcinoma in situ and invasive carcinoma. Whereas, overexpression of ANXA1 was related to unfavorable prognostic factors in

invasive cancer [50]. All these findings suggested that ANXA1 played dualistic roles and was involved in variable mechanisms associated with the advancement and proliferation in breast cancer. In the present study, APS alone especially couple to 5-FU significantly inhibited tumor growth in BALB/c mice after 14 days of treatment. All findings demonstrated that the inhibitory activity of APS towards 4T1-solid tumor probably attributed to the regulation of EGFR and ANXA1 apart from owing to the immunomodulatory role of APS. Most of the previous reports only evaluated the gene and protein expression of EGFR and ANXA1 *in vivo* in solid-tumor. Here, GFP-4T1 cells were further harvested and analyzed from subcutaneous tumors in all groups. Live/dead staining and CCK-8 analysis manifested remarkable decrease in cell viability after treatment with APS. For the sorted GFP-4T1 cells, it was identifiable that APS down-regulated the expression of EGFR protein and up-regulated the expression of ANXA1 protein using IF and flow cytometry analysis.

Conclusion

In summary, we identified a possible specific molecular mechanism of APS against 4T1 solid tumor using an integrated bioinformatics and experimental analysis, which indicated that EGFR and ANXA1 may be the potential therapeutic targets in breast tumor. In this study, a total of 201 DEGs were screened out, among which four common genes (EGFR, ANXA1, KIF14 and IGF1) participated the biological processes (cell cycle, cell proliferation and cell apoptosis) that were associated with the inhibitory effect of APS *in vitro* towards with breast cancer cell lines. Further, EGFR and ANXA1 were identified as hub genes that played important roles in the development of breast cancer. The down-regulated and up-regulated expression of EGFR and ANXA1 separately may be responsible for the anti-cancer mechanism of APS *in vivo* verified by multiple biological analyses. More breast cancer data profiles coupled to various algorithm theories and methods are needed to improve the accuracy of key genes, and provide further evidence to identify the targets of breast cancer and anti-cancer mechanisms of APS against breast cancer.

Abbreviations

APS: astragalus polysaccharide; qRT-PCR: quantitative real-time polymerase chain reaction**;** DEGs: differential expressed genes; PPI: protein-protein interaction; GO: Gene ontology; KEGG: Kyoto Encyclopedia of Genes and Genomes; EBI: European bioinformatics institute; DAVID: Database for Annotation, Visualization and Integrated Discovery; STRING: Search Tool for the Retrieval of Interacting Genes; BP: biological process; MF: molecular function; CC: cell component; TNBC: triple-negative breast cancer

Declarations

Author contributions

WL and KS designed the study; WL, XH and YL conducted the research; WL and XH analyzed the data; WL and XH wrote the manuscript; YL and KS revised the manuscript. All authors have read and agreed to the published version of the manuscript.

Funding

This work was supported by National Natural Science Foundation of China (32000977/31670978), Natural Science Foundation of Shandong Province (ZR2020QH188) and Health Commission of Shandong Province (2018WS064).

Data Availability Statement

All relevant data are within the manuscript.

Acknowledgments

We truly appreciate the contributions of all authors to this Original Research. We also thank all reviewers and editors who provided valuable and thoughtful comments.

Ethics approval and consent to participate

All animal care and experiments were conducted in accordance with regularity guidelines of the Guide for the Care and Use of Laboratory Animals of the Ministry of Health (China), and approved by the Ethics Committee of Weifang Medical University (Weifang, China, SCXK(Lu) 2019-0003).

Consent to publication

All the authors approved the publication of this manuscript.

Competing interests

The authors declare that they have no competing interests.

References

1. Bray F, Ferlay J, Soerjomataram I, Siegel RL, Torre LA, Jemal A. Global cancer statistics 2018: GLOBOCAN estimates of incidence and mortality worldwide for 36 cancers in 185 countries. Ca-a Cancer J Clin. 2018; 68: 394-424.

2. Yu Y, Shen M, Song Q, Xie J. Biological activities and pharmaceutical applications of polysaccharide from natural resources: A review. Carbohyd. Polym. 2018; 183: 91-101.
3. Yu J, Ji H, Yang Z, Liu A. Relationship between structural properties and antitumor activity of Astragalus polysaccharides extracted with different temperatures. Int. J. Biol. Macromol. 2019; 124: 469-77.
4. Guo S, Ma B, Jiang X, Li X, Jia Y. Astragalus Polysaccharides Inhibits Tumorigenesis and Lipid Metabolism Through miR-138-5p/SIRT1/SREBP1 Pathway in Prostate Cancer. Front. Pharmacol. 2020; 11: 598-605.
5. Wang B, Guo C, Liu Y, Han G, Li Y, Zhang Y, et al. Novel nano-pomegranates based on astragalus polysaccharides for targeting ER alpha-positive breast cancer and multidrug resistance. Drug Deliv. 2020; 27: 607-21.
6. Ye MN, Chen HF, Zhou RJ, Liao MJ. Effects of Astragalus polysaccharide on proliferation and Akt phosphorylation of the basal-like breast cancer cell line. J. Chin. Integr. Med. 2011; 9: 1339-46.
7. Guo L, Bai SP, Zhao L, Wang XH. Astragalus polysaccharide injection integrated with vinorelbine and cisplatin for patients with advanced non-small cell lung cancer: effects on quality of life and survival. Med. Oncol. 2012; 29: 1656-62.
8. Li W, Hu X, Wang S, Jiao Z, Sun T, Liu T, et al. Characterization and anti-tumor bioactivity of astragalus polysaccharides by immunomodulation. Int. J. Biol. Macromol. 2020; 145: 985-97.
9. Liu AJ Yu J, Ji HY, Zhang HC, Zhang Y, Liu HP. Extraction of a Novel Cold-Water-Soluble Polysaccharide from Astragalus membranaceus and Its Antitumor and Immunological Activities. Molecules. 2018; 23: 62-74.
10. Shi L. Bioactivities, isolation and purification methods of polysaccharides from natural products: A review. Int. J. Biol. Macromol. 2016; 92: 37-48.
11. Patel SJ, Sanjana NE, Kishton RJ, Eidizadeh A, Vodnala SK, Cam M, et al. Identification of essential genes for cancer immunotherapy. Nature. 2017; 548: 537-55.
12. Li W, Song K, Wang S, Zhang C, Zhuang M, Wang Y, et al. Anti-tumor potential of astragalus polysaccharides on breast cancer cell line mediated by macrophage activation. Mat. Sci. Eng. C-Mater. 2019; 98: 685-95.
13. Huang DW, Sherman BT, Lempicki RA. Systematic and integrative analysis of large gene lists using DAVID bioinformatics resources. Nat. Protoc. 2009; 4: 44-57.
14. Liao JH, Peng HS, Liu C, Li D, Yin YH, Lu B, et al. Dual pH-responsive-charge-reversal micelle platform for enhanced anticancer therapy. Mat. Sci. Eng. C-Mater. 2021; 118: 111527.
15. Hsieh CH, Lin CY, Hsu CL, Fan KH, Huang SF, Liao CT, et al. Incorporation of Astragalus polysaccharides injection during concurrent chemoradiotherapy in advanced pharyngeal or laryngeal squamous cell carcinoma: preliminary experience of a phase II double-blind, randomized trial. J. Cancer Res. Clin. 2020; 146: 33-41.
16. Huang WC, Kuo KT, Bamodu OA, Lin YK, Wang CH, Lee KY, et al. Astragalus polysaccharide (PG2) Ameliorates Cancer Symptom Clusters, as well as Improves Quality of Life in Patients with

Metastatic Disease, through Modulation of the Inflammatory Cascade. Cancers. 2019; 11: 1054.

17. Song J, Chen YM, He DH, Tan WH, Lv F, Liang B, et al. Astragalus Polysaccharide Promotes Adriamycin-Induced Apoptosis in Gastric Cancer Cells. Cancer Manag. Res. 2020; 12: 2405-14.
18. Zheng YJ, Ren WY, Zhang LN, Zhang YM, Liu DL, Liu YQ. A Review of the Pharmacological Action of Astragalus Polysaccharide. Front. Pharmacol. 2020; 11: 349.
19. Ponnusamy L, Natarajan SR, Thangaraj K, Manoharan R. Therapeutic aspects of AMPK in breast cancer: Progress, challenges, and future directions. BBA-Rev. Cancer. 2020; 1874: 188379.
20. Ajji PK, Binder MJ, Walder K, Puri M. Recombinant Balsamin induces apoptosis in liver and breast cancer cells via cell cycle arrest and regulation of apoptotic pathways. Process Biochem. 2020; 96: 146-56.
21. Pan Y, Zhang Y, Chen Q, Tao X, Liu J, Xiao GG. CTAB Enhances Chemo-Sensitivity Through Activation of AMPK Signaling Cascades in Breast Cancer. Front. Pharmacol. 2019; 10: 843-9.
22. Johnson J, Chow Z, Napier D, Lee E, Weiss HL, Evers BM, et al. Targeting PI3K and AMPK alpha Signaling Alone or in Combination to Enhance Radiosensitivity of Triple Negative Breast Cancer. Cells. 2020; 9: 1253-68.
23. Li W, Hu X, Wang S, Wang H, Parungao R, Wang Y, et al. Detection and Evaluation of Anti-Cancer Efficiency of Astragalus Polysaccharide Via a Tissue Engineered Tumor Model. Macromol. Biosci. 2018; 18: 1800223.
24. Miao K, Lei JH, Valecha MV, Zhang A, Xu J, Wang L, et al. NOTCH1 activation compensates BRCA1 deficiency and promotes triple-negative breast cancer formation. Nat. Commun.2020; 11: 3256-70.
25. Li T, Kon N, Jiang L, Tan M, Ludwig T, Zhao Y, et al. Tumor Suppression in the Absence of p53-Mediated Cell-Cycle Arrest, Apoptosis, and Senescence. Cell. 2012; 149: 1269-83.
26. Lu C, Klement JD, Yang D, Albers T, Lebedyeva IO, Waller JL, et al. SUV39H1 regulates human colon carcinoma apoptosis and cell cycle to promote tumor growth. Cancer Lett. 2020; 476: 87-96.
27. Delbridge ARD, Grabow S, Strasser A, Vaux DL. Thirty years of BCL-2: translating cell death discoveries into novel cancer therapies. Nat. Rev. Cancer. 2016; 16: 99-109.
28. Uhlen M, Oksvold P, Fagerberg L, Lundberg E, Jonasson K, Forsberg M, et al. Towards a knowledge-based Human Protein Atlas. Nat. Biotechnol. 2010; 28: 1248-50.
29. Xu T, Dong M, Li H, Zhang R, Li X. Elevated mRNA expression levels of DLGAP5 are associated with poor prognosis in breast cancer. Oncol. Lett. 2020; 19: 4053-65.
30. Behrens P, Brinkmann U, Wellmann A. CSE1L/CAS: Its role in proliferation and apoptosis. Apoptosis. 2003; 8: 39-44.
31. Tai CJ, Hsu CH, Shen SC, Lee WR, Jiang MC. Cellular apoptosis susceptibility (CSE1L/CAS) protein in cancer metastasis and chemotherapeutic drug-induced apoptosis. J. Exp. Clin. Canc. Res. 2010; 29: 110-8.
32. Nakahara I, Miyamoto M, Shibata T, Akashi-Tanaka S, Kinoshita T, Mogushi K, et al. Up-regulation of PSF1 promotes the growth of breast cancer cells. Genes Cells 2010; 15: 1015-24.

33. Toda H, Seki N, Kurozumi S, Shinden Y, Yamada Y, Nohata N, et al. RNA-sequence-based microRNA expression signature in breast cancer: tumor-suppressive miR-101-5p regulates molecular pathogenesis. Mol. Oncol. 2020; 14: 426-46.
34. Staff S, Isola J, Jumppanen M, Tanner M. Aurora-A gene is frequently amplified in basal-like breast cancer. Oncol. Rep. 2010; 23: 307-12.
35. Li L, Song Y, Liu Q, Liu X, Wang R, Kang C, et al. Low expression of PTEN is essential for maintenance of a malignant state in human gastric adenocarcinoma via upregulation of p-AURKA mediated by activation of AURKA. Int. J. Mol. Med. 2018; 41: 3629-41.
36. Justilien V, Fields AP. Ect2 links the PKC iota-Par6 alpha complex to Rac1 activation and cellular transformation. Oncogene. 2009; 28: 3597-607.
37. Simond AM, Muller WJ. In vivo modeling of the EGFR family in breast cancer progression and therapeutic approaches. Adv. Cancer Res. 2020; 147: 189-228.
38. Gao YS, Chen Y, Xu DY, Wang JJ, Yu GZ. Differential expression of ANXA1 in benign human gastrointestinal tissues and cancers. Bmc Cancer. 2014; 14: 1-12.
39. Jin Z, Jiang W, Wang L. Biomarkers for gastric cancer: Progression in early diagnosis and prognosis. Oncol. Lett. 2015; 9: 1502-8.
40. Garvey CM, Lau R, Sanchez A, Sun RX, Fong EJ, Doche ME, et al. Anti-EGFR Therapy Induces EGF Secretion by Cancer-Associated Fibroblasts to Confer Colorectal Cancer Chemoresistance. Cancers. 2020; 12: 1393-1407.
41. Maennling AE, Tur MK, Niebert M, Klockenbring T, Zeppernick F, Gattenloehner S, et al. Molecular Targeting Therapy against EGFR Family in Breast Cancer: Progress and Future Potentials. Cancers. 2019; 11: 1826-44.
42. Hsu JL, Hung MC. The role of HER2, EGFR, and other receptor tyrosine kinases in breast cancer. Cancer Metast. Rev. 2016; 35: 575-88.
43. Liao WS, Ho Y, Lin YW, Raj EN, Liu KK, Chen C, et al. Targeting EGFR of triple-negative breast cancer enhances the therapeutic efficacy of paclitaxel- and cetuximab-conjugated nanodiamond nanocomposite. Acta Biomater. 2019; 86: 395-405.
44. Mirsaeidi M, Gidfar S, Ann V, Schraufnagel D. Annexins family: insights into their functions and potential role in pathogenesis of sarcoidosis. J. Transl. Med. 2016; 14: 1-9.
45. Suh YE, Raulf N, Gaeken J, Lawler K, Urbano TG, Bullenkamp J, et al. MicroRNA-196a promotes an oncogenic effect in head and neck cancer cells by suppressing annexin A1 and enhancing radioresistance. Int. J. Cancer. 2015; 137: 1021-34.
46. Xue LY, Hu N, Song YM, Zou SM, Shou JZ, Qian LX, et al. Tissue microarray analysis reveals a tight correlation between protein expression pattern and progression of esophageal squamous cell carcinoma. Bmc Cancer. 2006; 6: 296-310.
47. Mussunoor S, Murray GI. The role of annexins in tumour development and progression. J. Pathol. 2008; 216: 131-40.

48. Maschler S, Gebeshuber CA, Wiedemann EM, Alacakaptan M, Schreiber M, Custic I, et al. Annexin A1 attenuates EMT and metastatic potential in breast cancer. Embo Mol. Med. 2010; 2: 401-14.
49. Shen DJ, Chang HR, Chen ZG, He JB, Lonsberry V, Elshimali Y, et al. Loss of annexin A1 expression in human breast cancer detected by multiple high-throughput analyses. Biochem. Bioph. Res. 2005; 326: 218-27.
50. Yom CK, Han W, Kim SW, Kim HS, Shin HC, Chang JN, et al. Clinical Significance of Annexin A1 Expression in Breast Cancer. J. Breast Cancer. 2011; 14: 262-8.

Figures

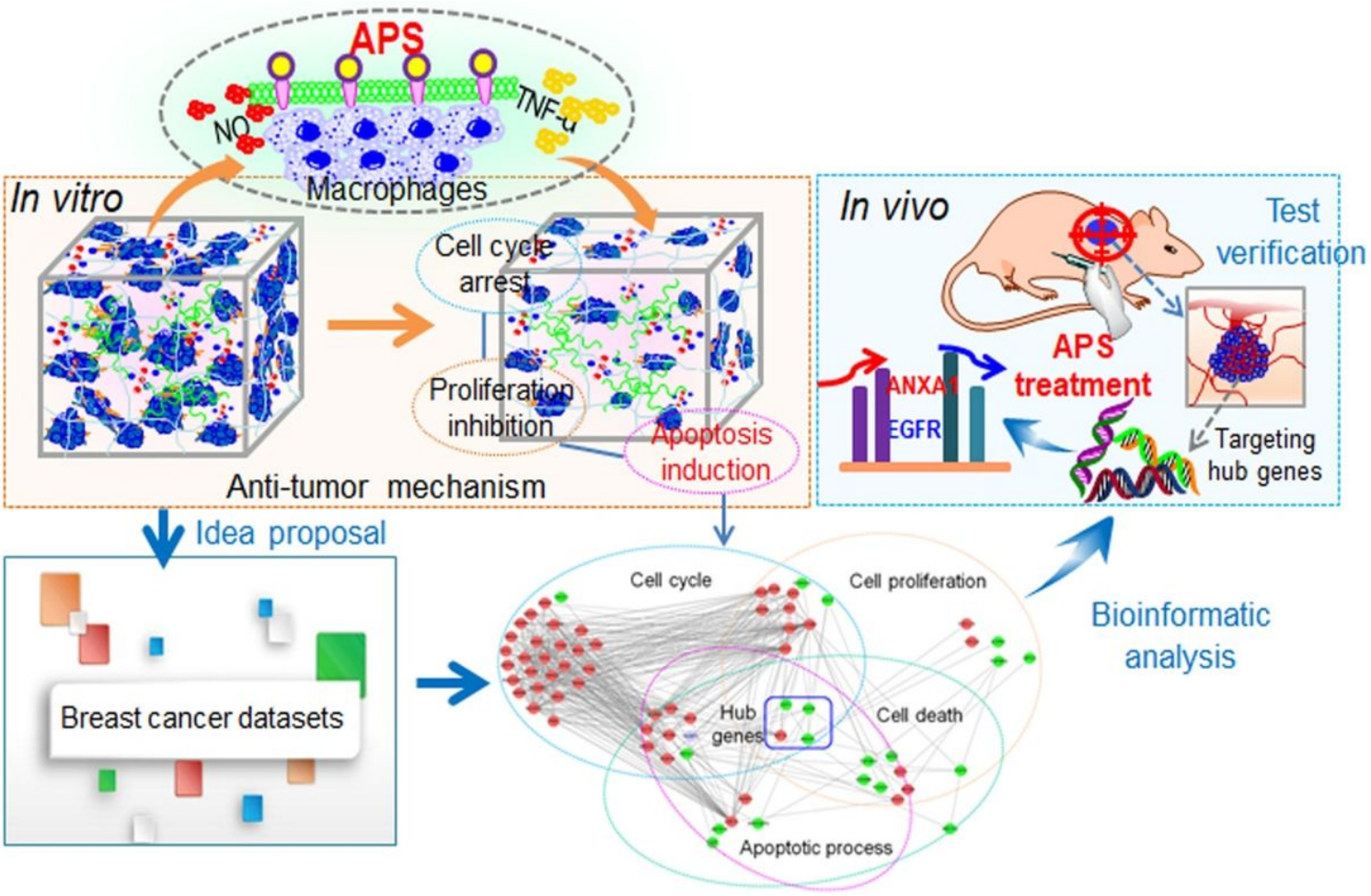

Figure 1

Schematic diagram of the identification of potential targets and anti-cancer molecular mechanism of APS.

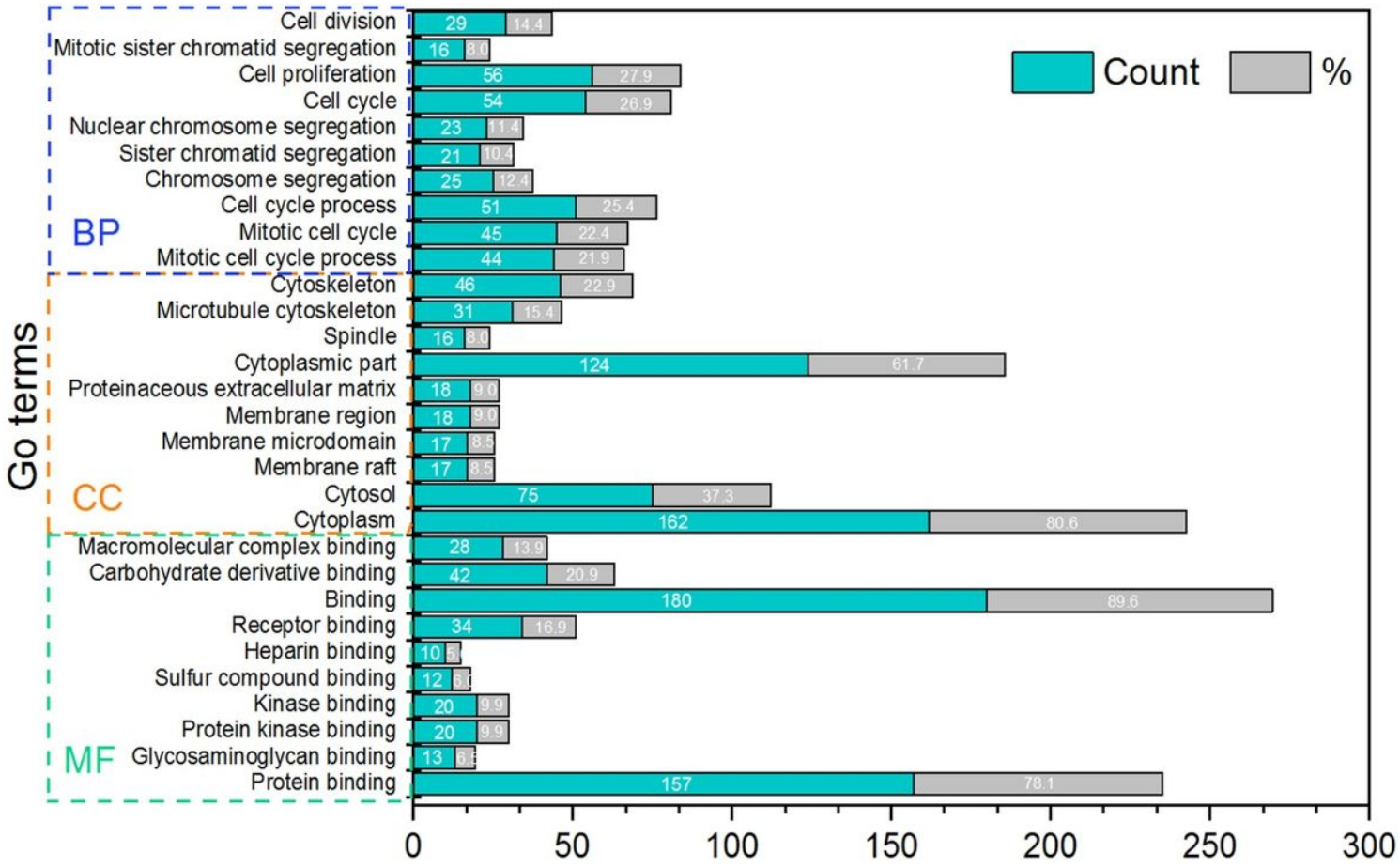

Figure 2

GO enrichment analysis results of DEGs.

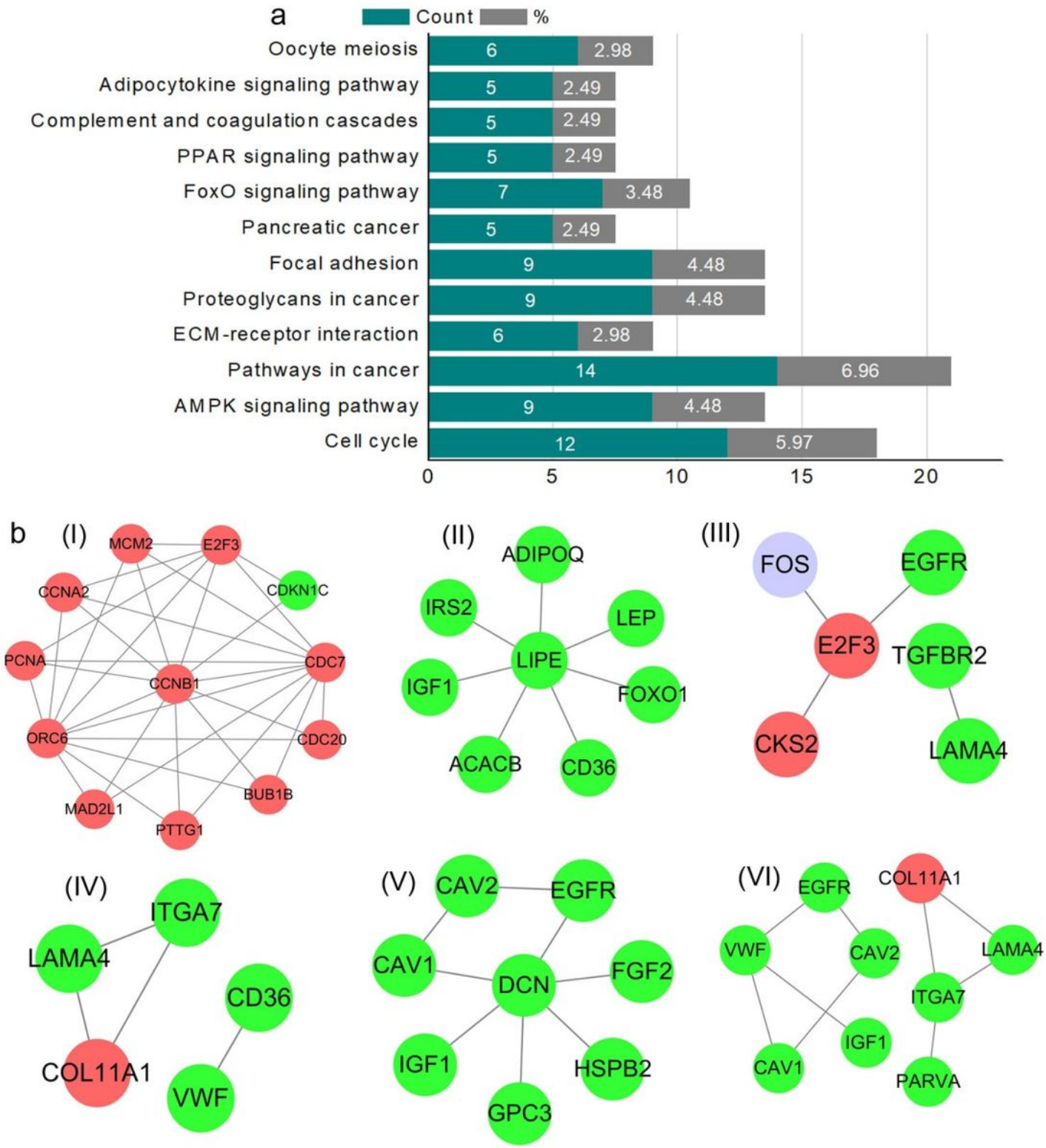

Figure 3

KEGG pathway enrichment and PPI subnetworks construction of DEGs. a KEGG pathway enrichment of 201 DEGs. The vertical axis is the pathway category and the horizontal axis is the count and percentage of DEGs in corresponding pathway. b Six subnetworks constructed of significant KEGG enrichment pathways of breast cancer. (I) Cell cycle; (II) AMPK signaling pathway; (III) Pathways in cancer; (IV) ECM-

receptor interaction; (V) Proteoglycans in cancer; (VI) Focal adhesion. Red color indicated up-regulated genes, green color indicated down-regulated genes, and blue color indicated non-co-regulated genes.

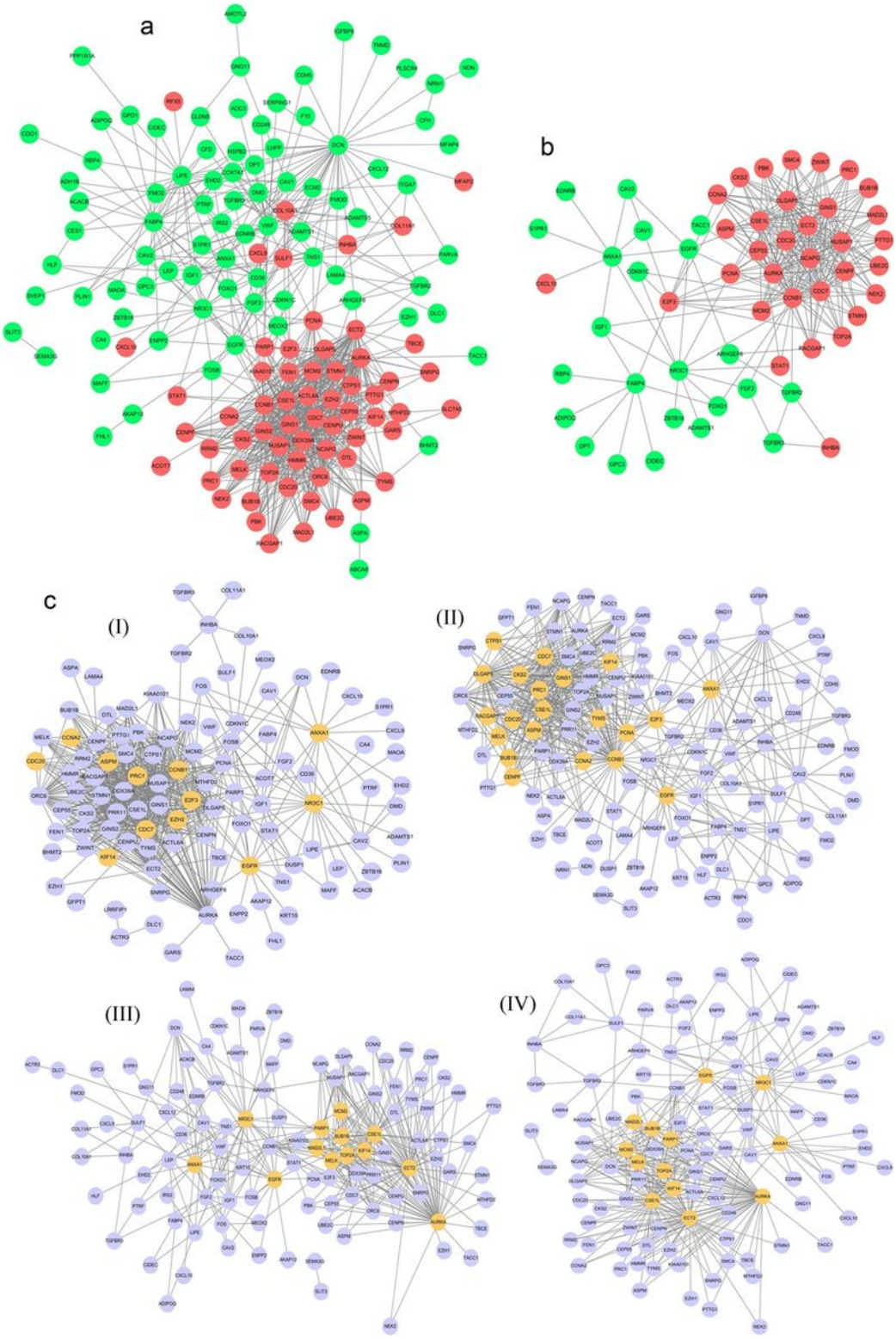

Figure 4

PPI interaction maps of DEGs. a Interactome of the 189 DEGs showing 146 nodes and 733 edges in the PPI network. The graph indicates genes and their interconnected interactions as nodes and edges respectively. Red color indicated up-regulated genes while green color indicated down-regulated genes. b

PPI network of DEGs involving in cell cycle, cell proliferation, apoptosis and death. c PPI networks of DEGs involved in 4 representative BP terms. (I) PPI network of DEGs involved in cell cycle; (II) PPI network of DEGs involved in cell proliferation; (III) PPI network of DEGs involved in cell death; (IV) PPI network of DEGs involved in apoptotic process. Orange color indicated DEGs with degree ≥ 10.

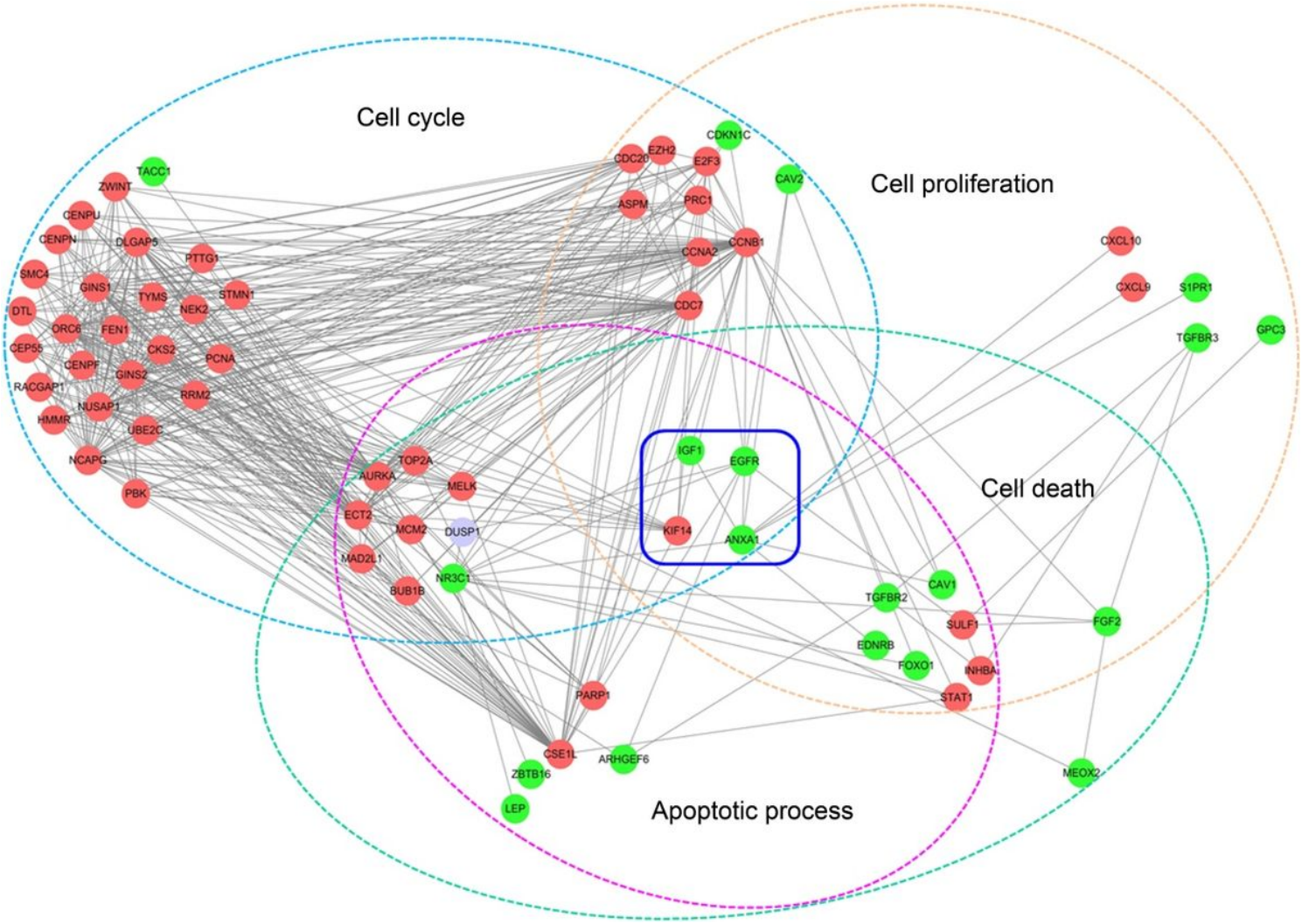

Figure 5

PPI networks constructed by DEGs from four BP terms. Green color indicated down-regulated genes, red color indicated up-regulated genes, and blue color indicated non-co-regulated genes.

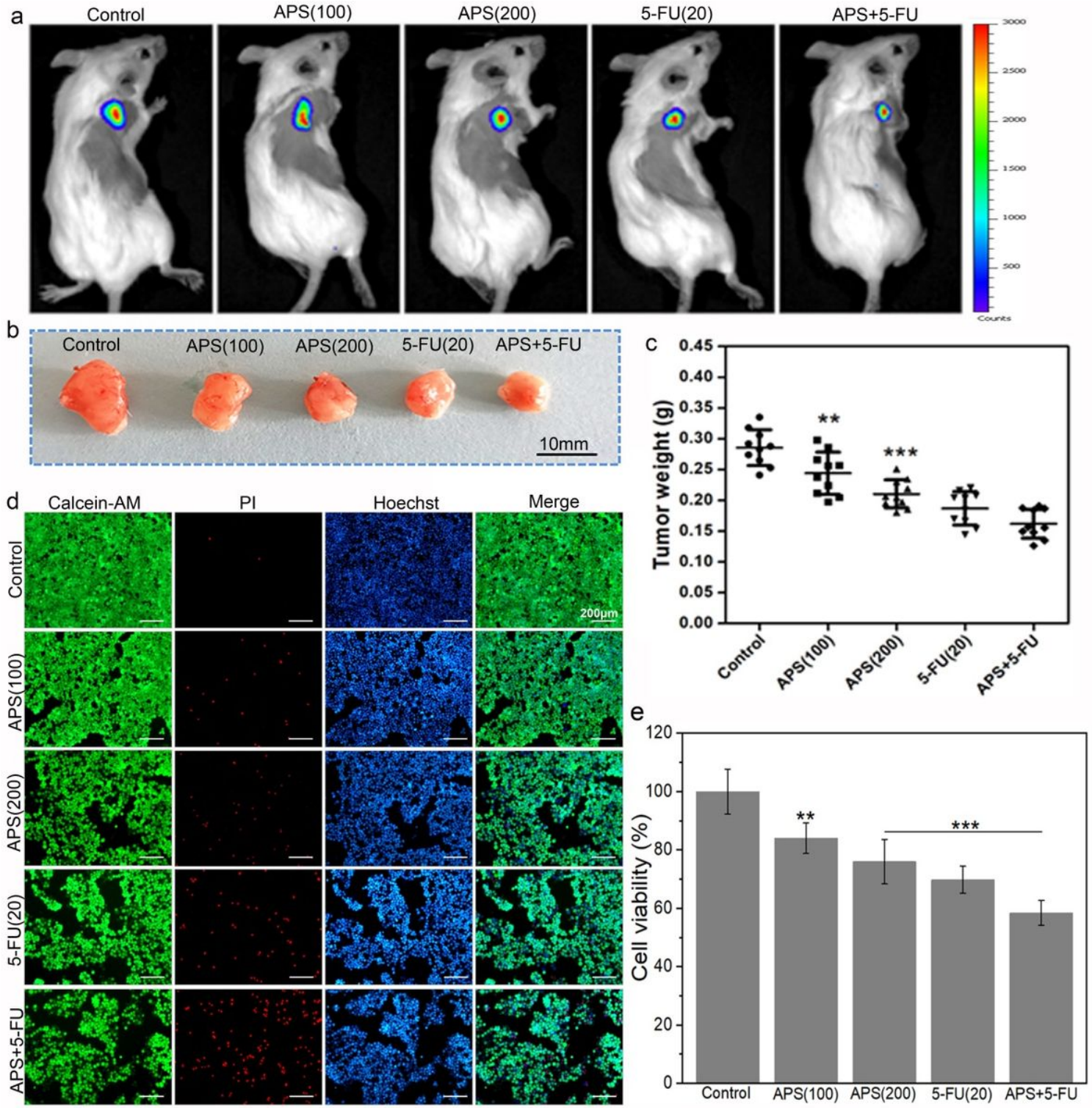

Figure 6

APS inhibited the growth of 4T1-solid tumor in BALB/c mice. a Typical live animal fluorescence imaging of subcutaneous 4T1-luc-solid tumor with drug intervention for 14 days. b Macroscopic appearance of GFP-4T1-solid tumor after treatment with drugs for 14 days. c Tumor weights in each group after the 14 days of drug administration. **P< 0.01, ***P< 0.001, compared with negative control group. d Cell viability of the sorted GFP-4T1 from in vivo tumor after drug intervention for 14 days using Live/dead staining.

Scale bar = 200 μm. e The viability of sorted GFP-4T1 cells were quantitatively assessed by CCK-8 (n=4). **P < 0.01, ***P < 0.001, compared with negative control group.

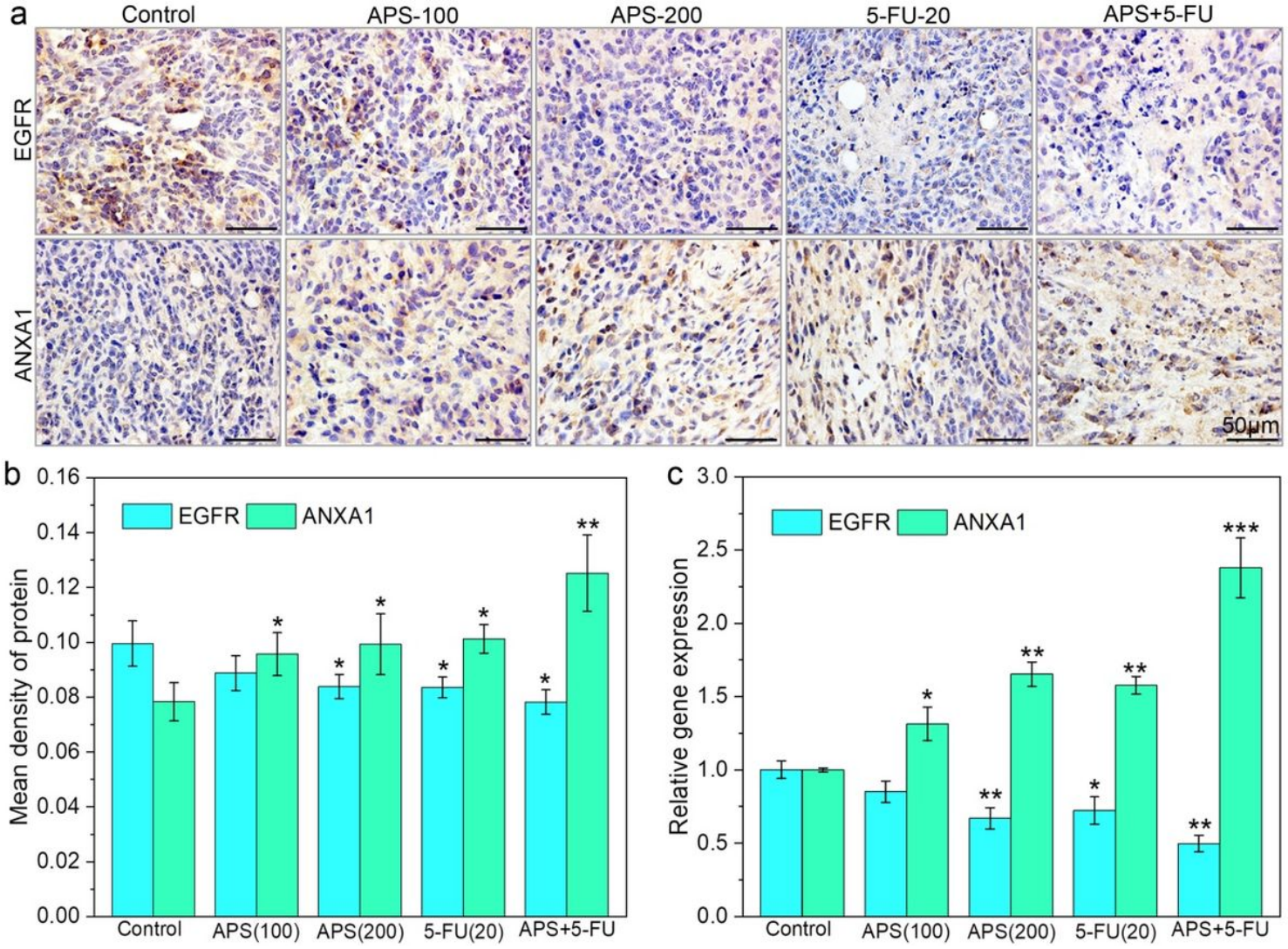

Figure 7

Effects of APS on the expression of ANXA1 and EGFR in 4T1 solid tumor of BALB/c mice. (A) Immunohistochemical assay of ANXA1 and EGFR protein after treatment with APS for 14 days, respectively. Scale bar = 50 μm; (B) Semiquantitative analysis of ANXA1 and EGFR expression. (C) PCR assay of ANXA1 and EGFR gene after exposure to APS for 14 days, respectively. *P<0.05, **P< 0.01, ***P< 0.001, compared with negative control group.

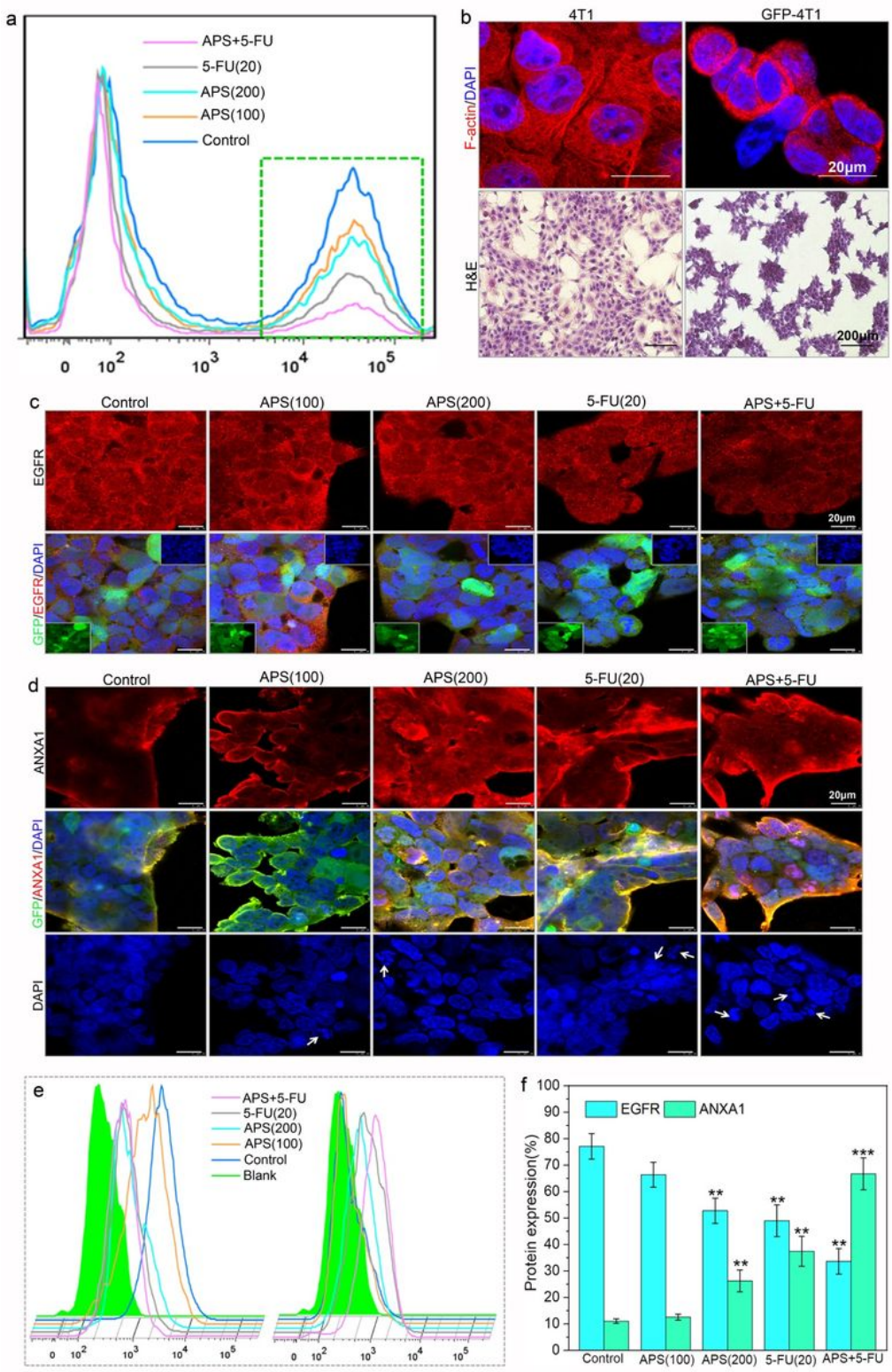

Figure 8

APS regulated the protein expressions of EGFR and ANXA1. a Cell sorting result of in vivo 4T1-solid tumor by flow cytometry. b Morphological changes between non-labeled and GFP-4T1 cells evidenced by H&E staining and F-actin immunofluorescence. c,d Immunofluorescence staining of EGFR and ANXA1 (red) in GFP (green) labeled 4T1 cells sorted from in vivo solid tumor after treatment with APS for 14 days, respectively. Scale bar = 20 μm. e EGFR and ANXA1 protein expression in GFP-4T1 cells by flow

cytometry intracellular staining. f Protein expression levels of EGFR and ANXA1in GFP-4T1 cells. *P<0.05, **P< 0.01, ***P< 0.001, compared with negative control group.